Effect of Stone-Wales Defects on transversely isotropic elastic properties of boron nitride nanotubes: a molecular dynamics study

Vijay Choyal, V. K. Choyal, and S. I. Kundalwal*
Applied and Theoretical Mechanics (ATOM) Laboratory, Discipline of Mechanical Engineering,
Indian Institute of Technology Indore, Simrol, Indore 453 552, India
kundalwal@iiti.ac.in,

Abstract: **- Current revolutions in the synthesis of boron nitride nanotubes (BNNTs) attracted researchers' attention to developing their nanocomposites. This is because BNNTs possess wide band gap, strong hardness, thermally and chemically stable, and excellent piezoelectric properties than carbon nanotubes. Besides, BNNTs have comparable mechanical and thermal properties compared to CNTs. As the first of its kind, this study reports the transversely isotropic elastic properties of pristine and Stone-Wales (SW) defected BNNTs within the framework of MDS using a Tersoff force field. This is achieved by imposing axial extension, twist, in-plane biaxial tension, and in-plane shear to the BNNTs. The study report that a higher density of SW defect affects profoundly the axial Young's modulus, shear modulus, plane strain bulk and in-plane shear moduli of BNNTs. The present fundamental study highlights the significant role played by SW defected BNNTs in determining their mechanical behaviours as reinforcements in multifunctional nanocomposites.**

Keywords: *Stone-Wales defects, Boron nitride nanotubes, Elastic properties, and Molecular dynamics simulations.*

I. Introduction

In the past decade, the discovery of carbon nanotubes (CNTs) done by Iijima [1] and their remarkable mechanical [2], [3], thermal [4] and electrical [5] properties have drawn a great deal of attention. After that, BNNTs revealed from its unexpected electromechanical [6], and thermal [7] properties. The structure of CNTs and BNNTs are similar from carbon (C) atoms are substituted by boron (B) and nitrogen (N) atoms [8]. Theoretical and experimental studies disclosed that BNNTs have a wide band gap (5.5 eV) regardless of their tube chirality and its morphology [9]. The chemical and thermal stability of BNNTs is higher than CNTs. Instead of that BNNTs demonstrated comparable mechanical properties to CNTs [10]. Such excellent properties make BNNTs a perfect material for many multifunctional applications like composite material [11], [12], hydrogen storage [13], transistors and optoelectronics[14].

Owing to some of the extraordinary properties of the BNNTs, attracted enormous attention to experimental and theoretical studies [15]. BNNTs are being fabricated by using well known techniques such as laser ablation [16] and arc discharge [17]. These synthesizing processes promote the presence of Stone-Wales (SW) defects [18]. however, defects in BNNTs bring controllably by irradiation process [19] which can make BNNTs for appropriate applications. Grown defects [20] play an important key factor to alter the unique mechanical properties of nanotubes. The SW defect is very significant in illustration of BNNTs and causes the presence of novel electronic levels in the essential band gap of the nanotube [21]. Hence, it is necessary to conduct a study on the impact of SW defects on the mechanical properties of BNNTs. BNNTs exposed to uniaxial loadings with several techniques such as tight-binding [22], molecular dynamics simulations (MDS) [23] [24] [25], and molecular mechanics (MM) [26]. Wang et al. [27] studied the stiffness, mechanical strength and failure strain of SW defected BNNTs. Their results revealed that SW defects expressively affect the mechanical properties of BNNTs for different loading condition via density functional theory (DFT) calculations. Roohi et al. [28] studied the effect of SW defects on the structural and electronic properties of BNNTs and they exposed that the band gap energy of BNNT increases under axial compression and decreases during axial tension. Huang et al. [18] studied the continuum model for SW transformation in BNNTs under tension. They observed that properties of BNNTs depend on the chirality and diameter of BNNTs respectively. Similarly, critical strain for armchair BNNTs was always higher than for zigzag BNNTs. Hu et al. [29] examined the electronic nanostructures of defected BNNTs under transverse electric fields by using DFT. The SW defect creates when B-N bond considering in between two hexagons and this B-N bond rotate by 90o about an axis that is perpendicular to the tube surface. After transformation, these B-N bond converted into B-B and N-N bonds. Four hexagonal cells as shown in Fig. 1 atom then transform into two pair of heptagonal and pentagonal 7/5/5/7, respectively [30].

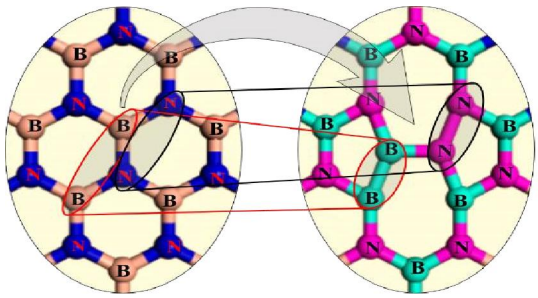

Fig. 1: Transformation of SW defects.

To the best of our knowledge, BNNTs are considered as isotropic for reviewing their mechanical properties for pristine as well as the influence of SW defects. This indeed provided us the inspiration for the present work. In the present study, MDS was performed to explore the effect

of SW defects on the transversely isotropic elastic properties along with fracture behavior of BNNTs.

II. MODELING

MDS is used to calculate the interatomic interaction in between atoms and molecules at the atomic level and this technique mainly used for simulation of nanostructures and nanomaterials. It involves the determination of the time evolution of a set of interacting atoms, followed by integration of the corresponding Newton's equation of motion step-by step [31]. In the present study, all MDS were completed by using open source software, Large-scale atomic/molecular massively parallel simulator (LAMMPS) [32], and molecular interactions of BNNTs were described in terms of three-body Tersoff potential force field [33].[23], [34], [35].

The step by step MDS were performed. Intially BNNTs nanostructured were prepared for both pristine and SW defected BNNTs, to maintain a steady state condition minimize there energy by using a conjugate gradient algorithm. Individually simulation was performed in the constant volume and temperature canonical (NVT) ensemble using a time step of 0.50 fs with a total time of 50.0 ps to equilibrate the BNNT nanostructures [36]. The Velocity Verlet algorithm was used to integrate Newton's classical equations of motion. Initially uniformly SW defect created in BNNTs, such as at 25 Å and 35 Å SW defect was formed, and the representation is for 25 Å length SW_1 and for 35 Å length SW_2. Schematics representation as shown in Fig.2.

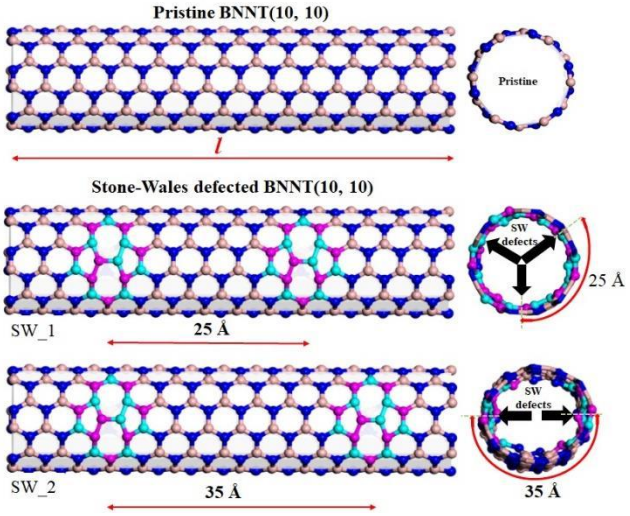

Fig. 2: Schematics representation of pristine and SW defected (10, 10) BNNT

To determine the five independent elastic moduli, four loading conditions (shown in Fig. 3) were applied to the BNNTs.

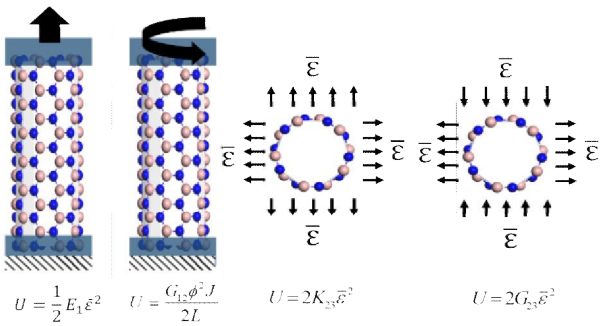

Fig. 3: Boundary conditions imposed on BNNTs: (a) Tensile, (b) Twisting, (c) In-plane biaxial tension, and (d) In-plane shear

Axial Young's modulus (E_1): From the slope of the stress-strain curve and distortion energy density determine the elastic constants. The axial stress was discolsed over the cross-sectional area of the BNNT; as follows:

$$\sigma_{axial} = \frac{1}{V}\frac{dE}{d\bar{\varepsilon}} \tag{1}$$

Where $\bar{\varepsilon}$ is the axial strain, σ_{axial} is the longitudinal stress, E is the strain energy in a BNNT, and V is the volume of a BNNT. Consequently, the strain energy density can be described as

$$U = \frac{1}{2}E_1\bar{\varepsilon}^2 \tag{2}$$

where U is the strain energy per unit volume and it is described by,

$$U = \frac{\Delta E}{Al} \tag{3}$$

where ΔE that increasing the potential energy of BNNT,$\bar{\varepsilon} = \Delta l/l$ is the axial strain of a BNNT, A describe cross-sectional area of a BNNT, and Δl describe changing length. Using the succeeding description, the major Poisson's ratio (ν_{12}) of a BNNT can be described,

$$\nu_{12} = -\frac{\bar{\varepsilon}_{22}}{\bar{\varepsilon}_{11}} \tag{4}$$

where $\bar{\varepsilon}_{22}$ and $\bar{\varepsilon}_{11}$ are the dispersed circumferential and axial strains.

Longitudinal shear modulus (G_{12}): A twisting moment with a constant rotation of 0.80°/ps of BNNT were applied for determining the G_{12} using the following relation.

$$U = \frac{G_{12}\phi^2 J}{2l} \tag{5}$$

where ϕ is the twisting angle and J is the polar moment of inertia; viz,

$$J = \frac{\pi}{32}\left[{D_o}^4 - {D_i}^4\right] \tag{6}$$

Plane-strain bulk modulus (K_{23}): A BNNT was exposed to the plane-strain condition. The plane strain bulk modulus (K_{23}) of a BNNT can be attained by using the subsequent relation [2], [3],

$$U = 2K_{23}\bar{\varepsilon}_{22} \tag{7}$$

In-plane shear modulus (G_{23}): A BNNT was exposed to in-plane shear at small strains in such way that its circular cross-section distorts into an elliptical shape. The in-plane shear modulus can be attained by using the subsequent definition [2], [3]:

$$U = 2G_{23}\bar{\varepsilon}_{22} \quad (8)$$

III. Results And Discussion

By using MDS determine elastic constants such as Young's modulus, Poisson's ratio and shear modulus of pristine and SW defected armchair (10, 10) BNNTs were compared with previous results [8], [23] and the evaluation was originated to be in the good agreement shown in Table 1.

Table 1: Five independent engineering constants of (10, 10) BNNTs

Case of BNNT	Engineering constants				
	E_1 (TPa)	ν_{12}	G_{12} (TPa)	K_{23} (TPa)	G_{23} (TPa)
SW_0	1.064	0.191	0.6617	0.301	0.173
Ref. [8]	1.064	0.190	0.6617	0.300	0.173
SW_1	0.910	0.173	0.5356	0.267	0.153
SW_2	0.879	0.159	0.4677	0.258	0.145

The Stress-strain curves of armchair (10, 10) BNNTs, as shown in fig. 4. Maximum stress reaches up to 110.02 GPa at strain 0.49-0.53. The slope of the curve obtained from the inset view of Fig. 4. The stress-strain curves are found to be in good agreement in the present study with those attained for pristine BNNTs [8], [36], [37]. The SW defected BNNTs (SW_1 and SW_2) were fractured at lower strain levels compared to SW_0. The Present study discloses that SW defected BNNTs, depicts the lower properties than pristine BNNTs. The trends of Poisson's ratios are originated to be same as those shown in Fig. 4. Although it is not shown here.

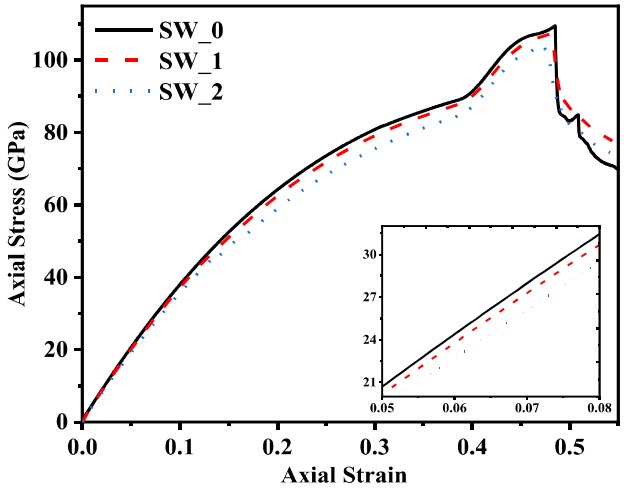

Fig. 4: Stress-strain curves for (10, 10) BNNTs

The variation of PE of armchair (10, 10) BNNTs as shown in Fig. 5. The SW_0 (pristine) shows higher PE energy compared to SW defects created for length 25 Å for SW_1 and 35 Å for SW_2.

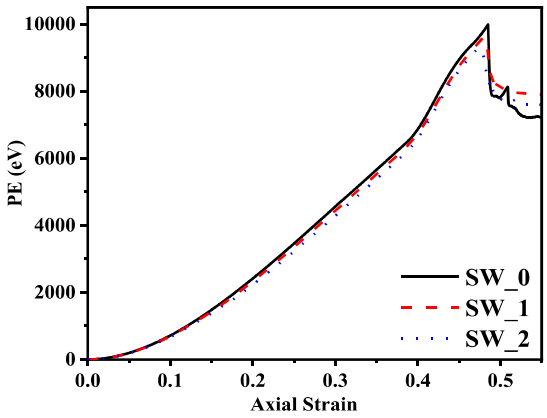

Fig. 5: Variation of PE of (10, 10) BNNTs

Subsequently, MDS performed BNNTs until they fractured under the torsional loading, in-plane bi-axial tension, and in-plane shear. In this work for the sake of brevity mechanical behaviour of a pristine and defected (10, 10) BNNTs considering for only axial tension. The value of G_{12}, K_{23}, and G_{23} obtained by strain-energy density-elastic constant relation are collected in Table 1. MDS snaps (Fig. 6) of BNNTs during uniform applied twist and demonstrate the change in the potential energy with the twisting angle for BNNTs. It shows that the BNNT first shows a flattening effect (Fig. 6a). The failure of BNNTs bonds starts at a critical angle of 35° shows in Fig. 6b and facture occur at an angle of 178° depict in Fig. 6c. The observed failure behaviour is comparable to previous studies [38].

he value of G_{12} of BNNTs reduces due to SW defects, by by 7% and 25% for SW_1 and SW_2, respectively. Fig. 7 illustrates the failure phenomena for in-plane bi-axial tension. The failure under in-plane loading starts at a strain value of 0.35 (Fig. 7a), it is a primary failure at PE 1100 eV. After that at the critical strain reaches up to 0.45 to 0.5, it is a secondary failure as shown in Fig. 7b. B-N bonds break permanently at critical strain 0.5 under in-plane loading. A comparable observation of BNNT under in-plane shear loading but not exposed here.

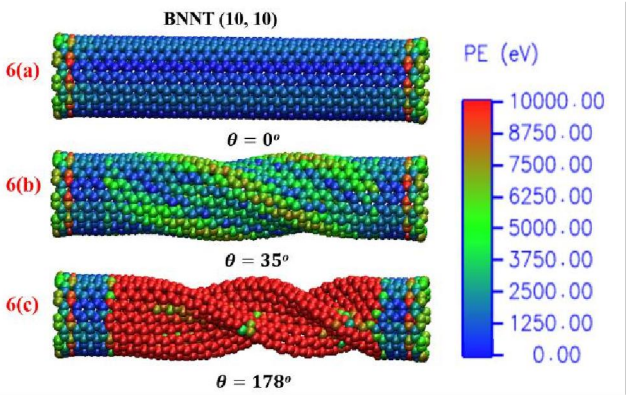

Fig. 6: Snapshot of twisting of pristine armchair (10, 10) BNNT.

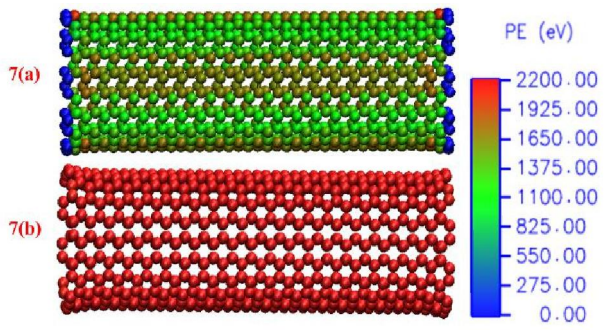

Fig. 7: Failure of BNNTs under in-plane bi-axial tension

IV. Conclusion

The elastic properties of pristine and SW defected BNNTs determine by using MDS. Our results reveal that the SW defected BNNTs diminishes elastic properties and their strength. The SW_2 (high density of SW defect) affects profoundly all the elastic properties of BNNTs. The present work illustrates that SW defects play a significant role in BNNTs which can be engineered and used to alter their properties of nanocomposite structures for multifunctional applications.

Acknowledgment

S.I.K. acknowledges the SERB ECR Award Grant (ECR/2017/001863) and the financial support by the DST-SERB and IIT Indore.

References

[1] S. Iijima, "Hellical microtubules of graphitic carbon," *Nature*, 1991.

[2] L. Shen and J. Li, "Transversely isotropic elastic properties of single-walled carbon nanotubes," *Phys. Rev. B*, vol. 69, no. 4, p. 45414, 2004.

[3] S. I. Kundalwal and V. Choyal, "Transversely isotropic elastic properties of carbon nanotubes containing vacancy defects using MD," *Acta Mech (2018) 229: 2571.*

[4] R. Kothari, S. I. Kundalwal, and S. K. Sahu, "Transversely isotropic thermal properties of carbon nanotubes containing vacancies," *Acta Mech.*, 2018.

[5] a Rochefort, P. Avouris, F. Lesage, and D. R. Salahub, "Electrical and mechanical properties of distorted carbon nanotubes," *Phys. Rev. B*, vol. 60, no. 19, pp. 13824–13830, 1999.

[6] N. G. Chopra and A. Zettl, "Measurement of the elastic modulus of a multi-wall boron nitride nanotube," *Solid State Communications*, vol. 105, no. 5. pp. 297–300, 1998.

[7] W. Sekkal, B. Bouhafs, H. Aourag, and M. Certier, "Molecular-dynamics simulation of structural and thermodynamic properties of boron nitride," *J. Phys. Condens. Matter*, vol. 10, no. 23, pp. 4975–4984, 1998.

[8] V. Choyal, V. K. Choyal, and S. I. Kundalwal, "Effect of atom vacancies on elastic and electronic properties of transversely isotropic boron nitride nanotubes: A comprehensive computational study," *Comput. Mater. Sci.*, vol. 156, pp. 332–345, Jan. 2019.

[9] X. Blase, A. Rubio, S. G. Louie, and M. L. Cohen, "Quasiparticle band structure of bulk hexagonal boron nitride and related systems," *Phys. Rev. B*, vol. 51, no. 11, pp. 6868–6875, 1995.

[10] S. S. Communications, "Pergamon," vol. 105, no. 5, pp. 297–300, 1998.

[11] R. Ansari and S. Ajori, "Molecular dynamics study of the torsional vibration characteristics of boron-nitride nanotubes," *Phys. Lett. Sect. A Gen. At. Solid State Phys.*, vol. 378, no. 38–39, pp. 2876–2880, 2014.

[12] V. Choyal and S. I. Kundalwal, "Interfacial characteristics of hybrid nanocomposite under thermomechanical loading," 2017.

[13] A. G. Arani, M. A. Roudbari, and S. Amir, "Nonlocal vibration of SWBNNT embedded in bundle of CNTs under a moving nanoparticle Elastic medium," *Phys. B Phys. Condens. Matter*, vol. 407, no. 17, pp. 3646–3653, 2012.

[14] D. Kumar, V. Verma, K. Dharamvir, and H. S. Bhatti, "Elastic moduli of boron nitride, aluminium nitride and gallium nitride nanotubes using second generation reactive empirical bond order potential," *Multidiscip. Model. Mater. Struct.*, vol. 11, no. 1, pp. 2–15, 2015.

[15] S. Sharma, R. Chandra, P. Kumar, and N. Kumar, "Effect of Stone-Wales and vacancy defects on elastic moduli of carbon nanotubes and their composites using molecular dynamics simulation," *Comput. Mater. Sci.*, vol. 86, pp. 1–8, 2014.

[16] J. Wang *et al.*, "Recent advancements in boron nitride nanotubes," *Nanoscale*, vol. 2, no. 10, p. 2028, 2010.

[17] N. G. Chopra *et al.*, "Boron Nitride Nanotubes," *Source Sci. New Ser. Chem. Phys. J. Chem. Phys. Methods En-zymol. J. Mol. Biol*, vol. 269107, no. 220, pp. 966–967, 1995.

[18] J. Song, H. Jiang, J. Wu, Y. Huang, and K. C. Hwang, "Stone-Wales transformation in boron nitride nanotubes," *Scr. Mater.*, vol. 57, no. 7, pp. 571–574, 2007.

[19] O. Lehtinen, E. Dumur, J. Kotakoski, A. V. Krasheninnikov, K. Nordlund, and J. Keinonen, "Production of defects in hexagonal boron nitride monolayer under ion irradiation," *Nucl. Instruments Methods Phys. Res. Sect. B Beam Interact. with Mater. Atoms*, vol. 269, no. 11, pp. 1327–1331, 2011.

[20] M. Griebel *et al.*, "A molecular dynamics study on the impact of defects and functionalization on the Young modulus of boron-nitride nanotubes," *Comput. Mater. Sci.*, vol. 45, no. 4, pp. 1097–1103, 2009.

[21] Y. Miyamoto, A. Rubio, S. Berber, M. Yoon, and D. Tománek, "Spectroscopic characterization of Stone-Wales defects in nanotubes," *Phys. Rev. B - Condens. Matter Mater. Phys.*, vol. 69, no. 12, 2004.

[22] H. F. Bettinger, T. Dumitrică, G. E. Scuseria, and B. I. Yakobson, "Mechanically induced defects and strength of BN nanotubes," *Phys. Rev. B - Condens. Matter Mater. Phys.*, vol. 65, no. 4, pp. 1–4, 2002.

[23] V. Verma, V. K. Jindal, and K. Dharamvir, "Elastic moduli of a boron nitride nanotube," *Nanotechnology*, vol. 18, no. 43, 2007.

[24] V. K. Choyal, V. Choyal, S. Nevhal, A. Bergaley, and S. I. Kundalwal, "Effect of aspects ratio on Young's modulus of boron nitride nanotubes: A molecular dynamics study," *Mater. Today Proc.*, 2019.

[25] V. Choyal, C. Ajay, K. Dasarath, and S. I. Kundalwal, "Role of grain boundaries on the thermal properties of carbon nanotubes," *Materials Today: Proceedings, 2019,ISSN 2214-7853.*

[26] R. Ansari, M. Faghihnasiri, S. Malakpour, and S. Sahmani, "Superlattices and Microstructures A DFT study of elastic and structural properties of (3 , 3) boron nitride nanotube under external electric field," *SUPERLATTICES Microstruct.*, vol. 82, pp. 90–102, 2015.

[27] H. Wang, N. Ding, X. Zhao, and C. L. Wu, "Defective boron nitride nanotubes : mechanical properties , electronic structures and failure behaviors," 2018.

[28] H. Roohi, M. Jahantab, and M. Yakta, "Effect of the Stone-Wales (SW) defect on the response of BNNT to axial tension and compression: A quantum chemical study," *Struct. Chem.*, vol. 26, no. 1, pp. 11–22, 2015.

[29] S. Hu, Z. Li, X. C. Zeng, and J. Yang, "Electronic structures of defective boron nitride nanotubes under transverse electric fields," *J. Phys. Chem. C*, vol. 112, no. 22, pp. 8424–8428, 2008.

[30] W. H. Moon and H. J. Hwang, "Molecular-dynamics simulation of structure and thermal behaviour of boron nitride nanotubes," vol. 431.

[31] M. Sammalkorpi, A. Krasheninnikov, A. Kuronen, K. Nordlund, and K. Kaski, "Mechanical properties of carbon nanotubes with vacancies and related defects," *Phys. Rev. B - Condens. Matter Mater. Phys.*, vol. 70, no. 24, pp. 1–8, 2004.

[32] S. Plimpton, "Fast Parallel Algorithms for Short -- Range

Molecular Dynamics," *J. Comput. Phys.*, vol. 117, no. June 1994. pp. 1–19, 1995.
[33] J. Tersoff, "Modeling solid-state chemistry: Interatomic potentials for multicomponent systems," *Phys. Rev. B*, vol. 39, no. 8, pp. 5566–5568, 1989.
[34] M. Santosh, P. Maiti, and A. K. Sood, "Elastic Properties of Boron Nitride Nanotubes and Their Comparison with Carbon Nanotubes," *J. Nanosci. Nanotechnol.*, vol. 9, no. 9, pp. 5425–5430, 2009.
[35] E. S. Oh, "Elastic properties of boron-nitride nanotubes through the continuum lattice approach," *Mater. Lett.*, vol. 64, no. 7, pp. 859–862, 2010.
[36] V. Choyal, V. K. Choyal, and S. I. Kundalwal, "Transversely Isotropic Elastic Properties of Vacancy Defected Boron Nitride Nanotubes Using Molecular Dynamics Simulations," *2018 IEEE 13th Nanotechnol. Mater. Devices Conf.*, pp. 1–4, 2018.
[37] D. T. Nguyen, "the Size Effect in Mechanics Properties of Boron Nitride Nanotube Under Tension," *Vietnam J. Sci. Technol.*, vol. 55, no. 4, pp. 475–483, 2017.
[38] J. M. Wernik and S. A. Meguid, "Atomistic-based continuum modeling of the nonlinear behavior of carbon nanotubes," *Acta Mech.*, vol. 212, no. 1–2, pp. 167–179, 2010.